

Comparison of static and fatigue interlaminar testing methods for continuous fiber reinforced polymer composites

Szebényi Gábor, Magyar Balázs, Iványicki Tamás

This accepted author manuscript is copyrighted and published by Elsevier. It is posted here by agreement between Elsevier and MTA. The definitive version of the text was subsequently published in [Polymer Testing, 63, 2017, DOI:

[10.1016/j.polymertesting.2017.08.033](https://doi.org/10.1016/j.polymertesting.2017.08.033)]. Available under license CC-BY-NC-ND.

Comparison of static and fatigue interlaminar testing methods for continuous fiber reinforced polymer composites

Gábor SZEBÉNYI^{1,2*}, Balázs MAGYAR¹, Tamás IVÁNYICKI¹

¹ Department of Polymer Engineering, Faculty of Mechanical Engineering, Budapest University of Technology and Economics, Műegyetem rkp. 3., H-1111 Budapest, Hungary

² MTA–BME Research Group for Composite Science and Technology, Műegyetem rkp. 3., H-1111 Budapest, Hungary

* corresponding author: szebenyi@pt.bme.hu, +36-1-463-1466

E-mail addresses:

Gábor SZEBÉNYI – szebenyi@pt.bme.hu

Balázs MAGYAR – embalazs93@gmail.com

Tamás IVÁNYICKI- ivanyicki.t@gmail.com

Abstract

Two different interlaminar fatigue testing methods have been compared by testing a carbon fiber reinforced epoxy (CF/EP) composite and a carbon fiber/multiwalled carbon nanotube reinforced epoxy (CF/MWCNT/EP) hybrid nanocomposite. The first, conventional fatigue testing method was the end-notched flexure (ENF) test, which was used as a reference. The second, novel technique was the fatigue interpretation of the double-notch shear (DNS) test. Both tests have been performed with static and cyclic loading to compare the evaluated

properties of the different systems, the effect of transition from cyclic to fatigue loading and to demonstrate if the complex ENF test can be replaced by the simpler DNS test.

The test results showed the slight beneficial effect of the nanoreinforcement in both static and cyclic load conditions, and the possibility to use the DNS test for fatigue testing of continuous fiber reinforced composites. The SEM micrographs taken of the fracture surfaces of the composites after the different interlaminar tests provide valuable data on the interlaminar failure phenomena of hybrid nanocomposites in both static and fatigue loading conditions.

Keywords

interlaminar properties, fatigue, fracture analysis

1. Introduction

Nowadays continuous fiber reinforced polymer composites are attracting increasing attention in safety-critical applications, like the aerospace and the transportation industry. Due to their outstanding mechanical properties, these lightweight materials can be loaded up to a high level not only in static, but in cyclic load conditions. The catastrophic failure of a composite is caused in most cases by the synergy of multiple failure processes: fiber breakage, matrix fracture, fiber-matrix debonding/pullout and delamination [1]. While in the case of dynamic loading the first two processes are dominant, in the case of cyclic loading, interfacial/interlaminar failure processes play greater role [2-5].

For the comparison of different matrix materials containing novel additives, it is essential to characterize the interfacial properties not only in the case of static [6-8] but also in the case of dynamic loading [9-10]. For the characterization of these properties, strength and toughness parameters need to be measured, which can be done by different methods, with delamination artificially initiated [11-12] in most cases. For static testing the two most common methods are the short beam shear test [13-14] and the double-notched interlaminar shear test [15-16]. In the case of short beam shear, delamination forms and propagates during the bending test of a relatively thick specimen in the three-point bending setup, while in the case of the double-notched interlaminar shear test, interlaminar stress is introduced by the compressive or tensile loading parallel to the interface. Fatigue properties are mostly characterized with the ENF [17-19] test, which is similar to the short beam shear method used in the static setup, but delamination does not start at the free edge of the specimen but at an artificial initial delamination front. Since artificial delamination has to be introduced and compliance calibration has to be performed, the ENF test is complex.

The aim of this study is to introduce the DNS interlaminar test as an easy way to characterize not only static but cyclic interlaminar properties, to validate the results and compare them to ENF test results, and check the correlation between them.

2. Materials and methods

2.1. Materials

IPOX ER 1010 (IPOX Chemicals, Budapest, Hungary) DGEBA-based epoxy resin (viscosity: 800-1200 mPa·s at 25°C, epoxy equivalent: 175-190 g/equiv) with IPOX MH

3124 amine-based curing agent (viscosity: 40-70 mPa·s at 25°C, amine value: 450-470 mg KOH/g) was used as the matrix of the composite laminates. The mixing weight ratio of the resin and the curing agent was 100:35, according to the producer's specifications.

As nanosized reinforcement, Bayer Baytubes C150HP (Bayer, Leverkusen, Germany) multiwalled carbon nanotubes (MWCNTs) were used. The nanotubes were produced in a CVD based catalytic process resulting in an average outer diameter between 13–16 nm, length above 1 µm and carbon purity above 99%, according to the manufacturer.

As fiber reinforcement, PX35FBUD0300 (Zoltek Zrt., Nergesújfalu, Hungary) unidirectional carbon weave (surface weight 309 g/m²), consisting of Panex35 50k rovings was used.

The test specimens consisted of 6 layers of unidirectional carbon weave placed in the 0° direction. The composites were produced by hand lay-up followed by vacuum pressing for 2 hours in a 0.5 bar vacuum at room temperature. The post-curing of the samples was performed in a Heraeus UT 20 (Heraeus, Hanau, Germany) drying oven at 60°C for 4 hours. The pre-crack of the ENF specimens was generated by a 10 µm thick polyethylene terephthalate (PET) film treated with Formula Five mould release wax (Rexco, Conyers, USA) laminated between the reinforcing layers. The two notches required for the DNS tests were prepared with a Mutronic Diadisc (Mutronic, Rieden am Forggensee, Germany) diamond disc cutter.

2.2. Experimental

The static ENF tests were performed on 11-11 standard 250 mm long, 25 mm wide, 3 mm thick specimens with an initial crack size of 50 mm, with an Instron 5985 (Norwood, USA) universal tester equipped with standard three-point bending fixtures. The test speed was 5 mm/min, the support span was 200 mm. Crack propagation was tracked with a Mitutoyo

(Takatsu-ku, Japan) optical microscope. The Mode II interlaminar fracture toughness was evaluated according to specifications of the standard [19]. Before each test, the specimens were loaded up to the first crack jump at 0.5 mm/min crosshead speed to achieve a natural pre-crack. The precrack length was checked for each specimen. Specimens above 4 mm pre-crack length could indicate impurities in the middle matrix film, based on preliminary test results, therefore were discarded to be able to work with a homogeneous specimen group for the comparison of the test methods.

The cyclic ENF tests were performed on 21-21 specimens identical to the static test specimens with an Instron Labtronic 8800 fatigue tester with the same fixtures. After the formation of the natural pre-crack, the specimens were loaded in load-controlled operation with a sinusoidal waveform. The tests were performed with 5 Hz pulsating sinusoidal loading. The maximal forces used during the tests were set to 70, 75, 80 and 85% of static failure loads. The load ratio (maximum load/minimum load) was 10. From the ENF test results recorded by the data acquisition unit, the dynamic spring compliance was calculated at each recorded cycle from the maximum value of the deflection divided by the corresponding maximum load of the specimen. By plotting the dynamic spring compliance, the stiffness change of the specimen during the crack propagation can be easily visualized.

The static DNS tests were performed on 11-11 standard 150 mm long, 12.5 mm wide, 3 mm thick specimens with notches on opposite sides 6.4 mm from each other in tensile setup with a Zwick Z020 (Zwick, Ulm, Germany) universal tester equipped with self-aligning tensile grips to minimize the effect of grip misalignment. The test speed was 2 mm/min. The Mode II interlaminar shear strength was evaluated according to specifications of the standard [15].

The cyclic DNS tests were performed on 21-21 specimens identical to the static test specimens with an Instron Labtronic 8800 fatigue tester with the same fixtures. The specimens were loaded in load-controlled operation with a sinusoidal waveform at a frequency of 5 Hz. The maximal stresses used during the tests were set to 70, 75, 80 and 85% of the static failure loads. The load ratio (maximum load/minimum load) was 10.

The test setup of each test is presented in Fig. 1.

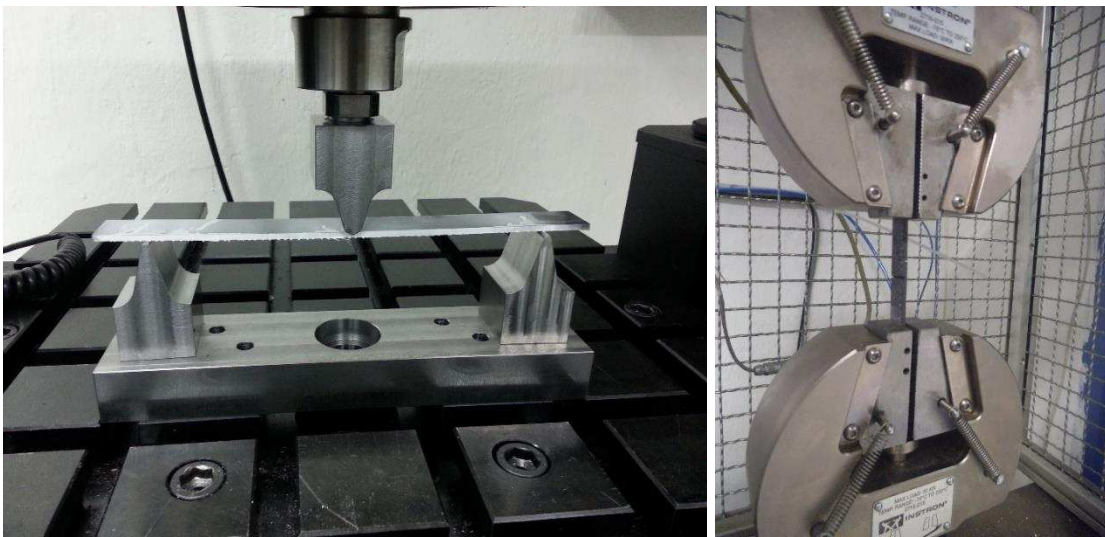


Fig. 1. Test setup of the ENF (left) and DNS tests (right)

The scanning electron microscope (SEM) micrographs were taken by a JEOL JSM-6380LA (Tokyo, Japan) scanning electron microscope. The samples were gold spur coated with a JEOL FC-1200 device to achieve a thin conductive layer on their surface.

3. Results and discussion

The results of the static interlaminar tests are presented in Table 1.

Composite type	Mode II interlaminar fracture toughness [kJ/m ²]	Interlaminar shear strength [MPa]
CF/EP	2.20±0.3	21.8±2.1
CF/MWCNT/EP	2.62±0.4	24.5±2.3

Table 1. Results of the static interlaminar tests

The slight beneficial effect of the MWCNT filling of the matrix could be observed in both the Mode II interlaminar fracture toughness values obtained from the ENF tests and the interlaminar shear strength values obtained from the DNS tests. Because of the overlapping confidence intervals, to check the significance of the difference between the measured values two-sample t-tests were performed. The results of the statistical tests showed that the differences between the hybrid nanocomposites and the traditional composites are significant at a 95% level of significance. This can be explained by the interlaminar toughening effect of well-dispersed nanofillers, which help to achieve a more uniform load distribution along the crack and hinder crack propagation.

Representative SEM micrographs of the tested ENF and DNS specimens are presented in Fig. 2 and Fig. 3 respectively. Comparing the micrographs of the ENF and DNS fracture surfaces, the main difference is that in the case of the ENF specimens, the propagating crack left a clearly periodic fracture surface texture, while in case of the DNS tests the matrix surface is smooth, showing that the main failure mode was the fiber-matrix debonding at the catastrophic fracture. Comparing the micrographs of the ENF fracture surfaces of the two samples, the main difference is in the distance between the parallel lines corresponding to the crack jumps, which in the case of the hybrid nanocomposite is much larger. According to this, we can assume that during the test higher energy had to be accumulated for the crack to propagate in the stronger matrix, resulting in longer micro-jumps. This supports the measured improvement in the static interlaminar mechanical properties caused by the interlaminar toughening effect of the nanofillers.

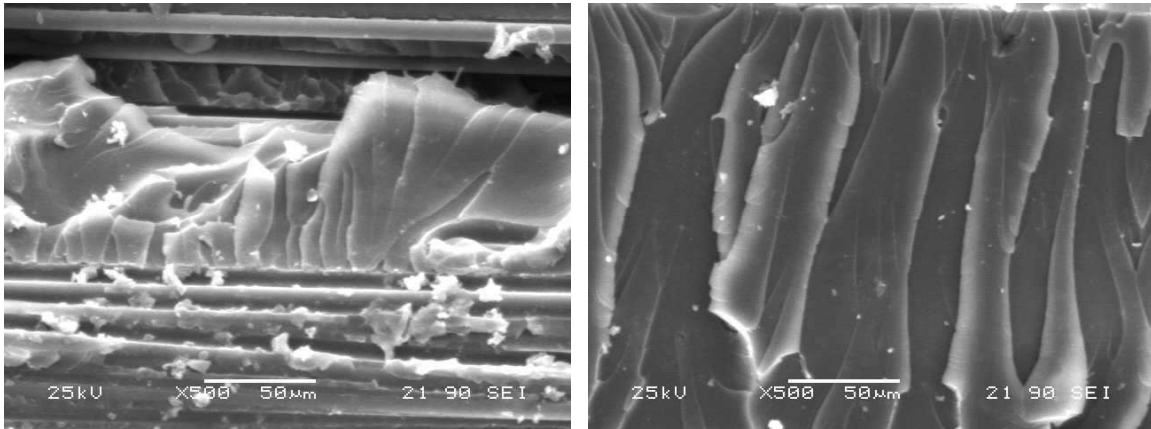


Fig. 2. SEM micrographs of the fracture surfaces of the static ENF specimens (CF/EP – left, CF/MWCNT/EP – right)

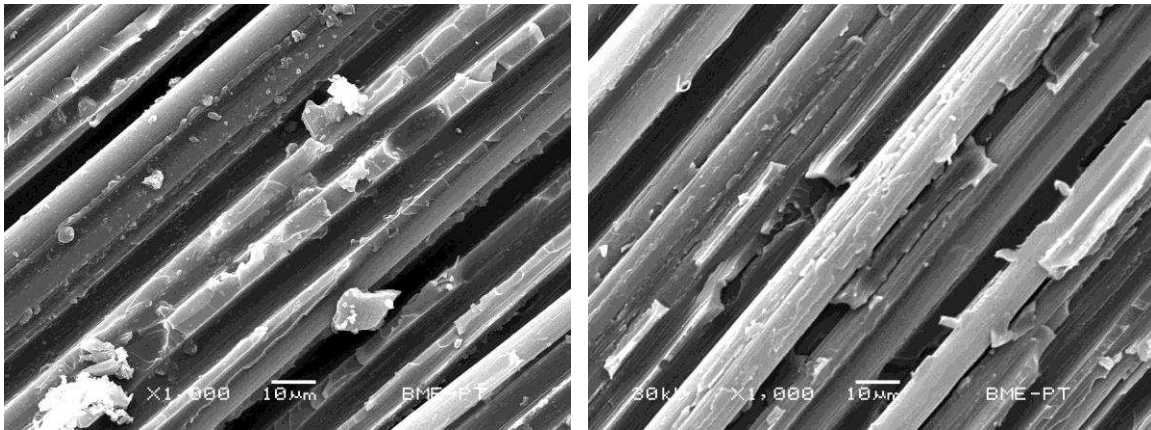


Fig. 3. SEM micrographs of the fracture surfaces of the static DNS specimens (CF/EP – left, CF/MWCNT/EP – right)

A characteristic dynamic bending compliance plot of one of the tested CF/EP composites ENF fatigue tests specimens is presented in Fig. 4 (the shape of the curve of the CF/EP/MWCNT hybrid composite is similar).

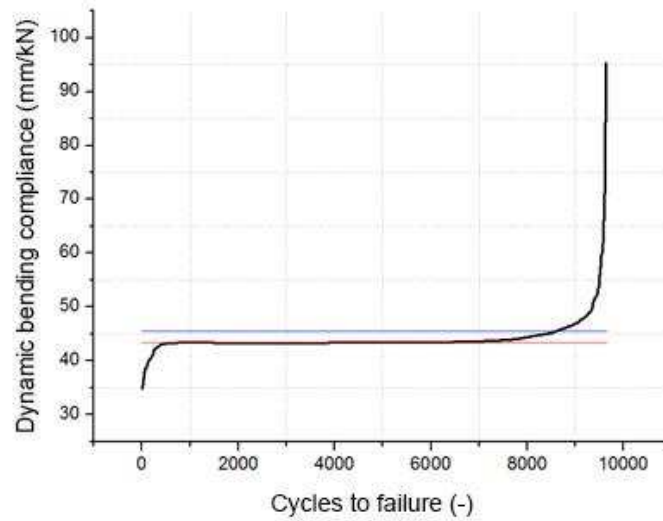


Fig. 4. Characteristic dynamic bending compliance – cycle number plot of the ENF fatigue tests

Fig. 4 shows that after the first few cycles dynamic bending compliance reaches an equilibrium state where spring compliance is almost a constant value. After reaching a critical crack concentration, bending compliance deviates from this value and a catastrophic failure occurs. During the evaluation of the results, an increase of 5% of the steady state spring compliance (red line in Fig. 4) was used as a failure criterion (blue line in Fig. 4). The S-N curves composed of the maximum of the interlaminar shear stress values and failure cycle numbers are presented in Fig. 5. Besides the individual results, the figure also shows the fitted regression curves and the 90% confidence intervals.

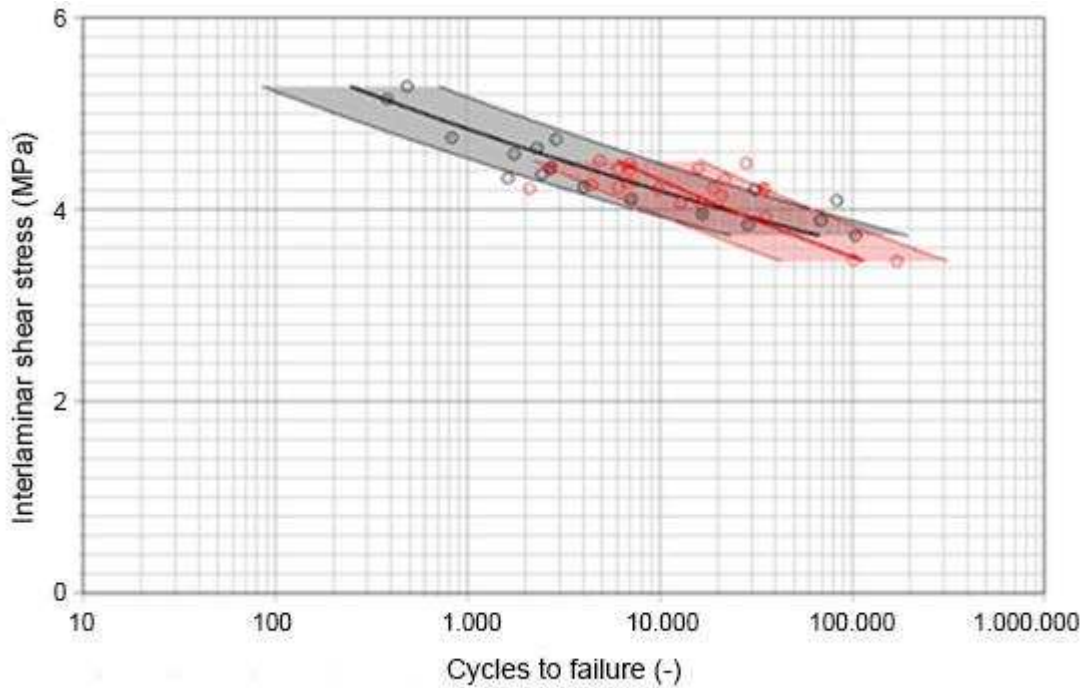


Fig. 5. S-N curves of the ENF fatigue tests (CF/EP – red, CF/MWCNT/EP – black)

Fig. 5 shows that the inclusion of MWCNTs had only a marginal effect on fatigue behavior: while the fitted S-N curve is slightly steeper, the confidence intervals are completely overlapping. This can be explained with the different failure method compared to the static test. In the static test, only the main crack is propagating, while in the case of the fatigue test, the complex structure of the composite leads to the formation of numerous micro-cracks in the whole specimen. This negative effect cancels out the toughening effect of the nanofiller. The SEM micrographs (Fig. 6) show the different failure behavior of the two systems. In the case of the CF/EP composite the fracture surface is similar to the fracture surface of the static test. In the case of the CF/MWCNT/EP composite the fracture surface is much more complex. The parallel ridges representing the steady crack propagation are still present, but areas showing ductile behavior, where the crack has to change its path numerous times, are

dominant. These complex areas can be also formed when more cracks meet during their propagation. This can be the root cause of the cancelling out of the toughening effect of the nanofillers.

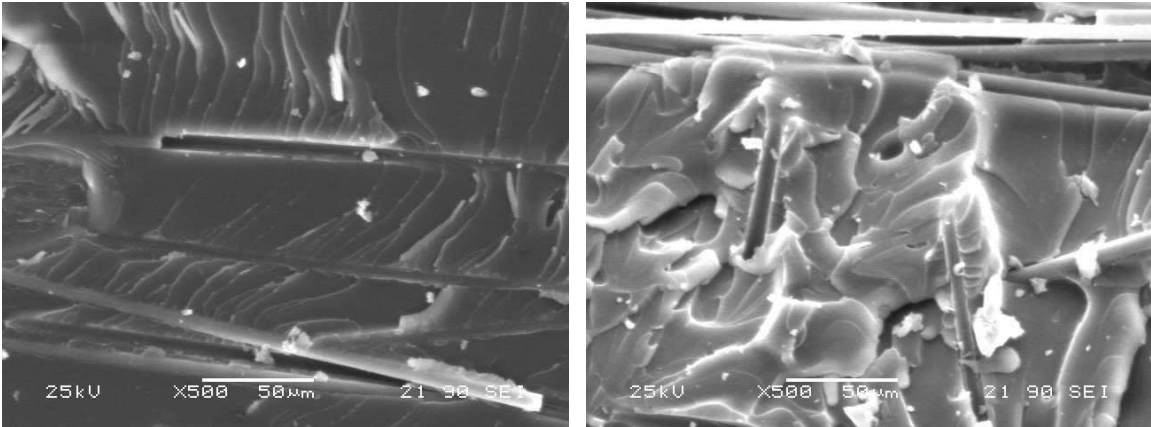


Fig. 6. SEM micrographs of the fracture surfaces of the ENF fatigue specimens (CF/EP – left, CF/MWCNT/EP – right)

After the fatigue test, each failed specimen was retested in static loading to measure their remaining static bending compliance. The bending compliance values as a function of the measured crack lengths are presented in Fig. 7 with the corresponding regression curves and 90% confidence intervals.

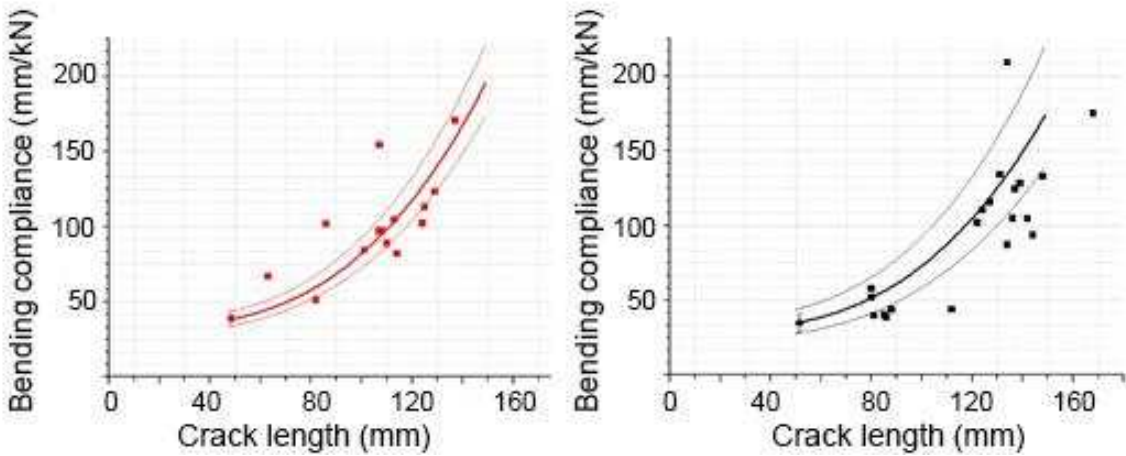


Fig. 7. Remaining bending compliance of the failed ENF fatigue specimens (CF/EP – left, CF/MWCNT/EP – right)

Fig. 7 shows that the fitted curve moved in the direction of higher crack lengths, which indicates that in the case of the same structural damage (crack length), MWCNT-reinforced composites were stiffer, therefore the hybrid structure is more fault-tolerant. This correlates with the SEM micrographs. There can be more smaller cracks still present in the MWCNT containing composites, but they are unable to propagate and negatively effect the stiffness of the composite in the static loading performed after the fatigue tests.

The specimens of the DNS fatigue tests showed a catastrophic failure at the end of the tests.

The fitted S-N curves and 90% confidence intervals are presented in Fig. 8.

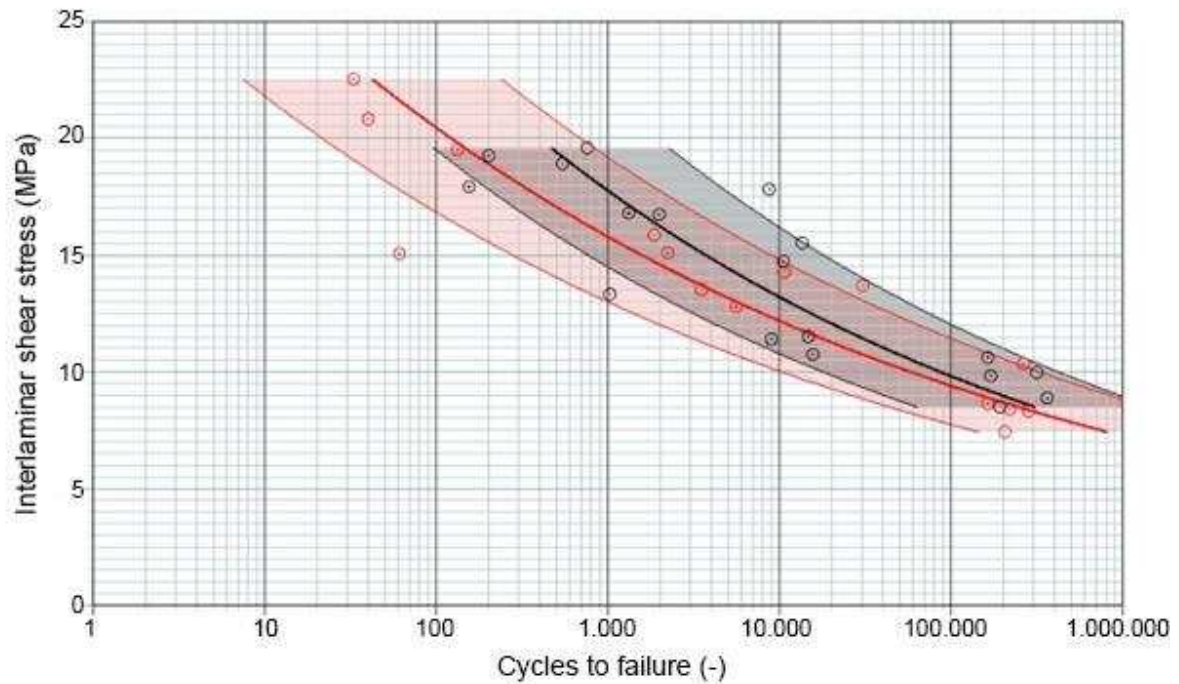


Fig. 8. S-N curves of the DNS fatigue tests (CF/EP – red, CF/MWCNT/EP – black)

Fig. 8 shows that while the confidence intervals are overlapping, the curve of the MWCNT-reinforced hybrid composites moved towards the higher failure cycle region, showing higher fatigue resistance. The largest difference is at the high load level range (approximately above 10 MPa maximum interlaminar shear stress), where the MWCNT-filled composites performed much better. The two average curves are not parallel, at the range of the lower cycles to failure there is a significant difference between the slopes of the two curves. The higher slope of the curve corresponding to the MWCNT-filled system suggests that the MWCNTs help to withstand more fatigue cycles at a given high interlaminar shear stress level. This can be caused by the toughening, crack-pinning effect of the nanotubes and their stiffening effect on the matrix, demonstrated in the previous tests. At the highest cycles to failure range, above 100.000 cycles, they converge asymptotically at the high cycles to failure range.

In the SEM micrographs of the fracture surfaces (Fig. 9) significant differences can be pointed compared to the static test. Finely fractured matrix particles are present between the reinforcing carbon fibers. This shows that the micro-cracks propagated by small microscale crack jumps at the interface. Comparing the length of the microscale crack jumps a similar phenomenon can be observed. The texture of the fractured matrix shows a more ductile fracture in case of the MWCNT reinforced composite.

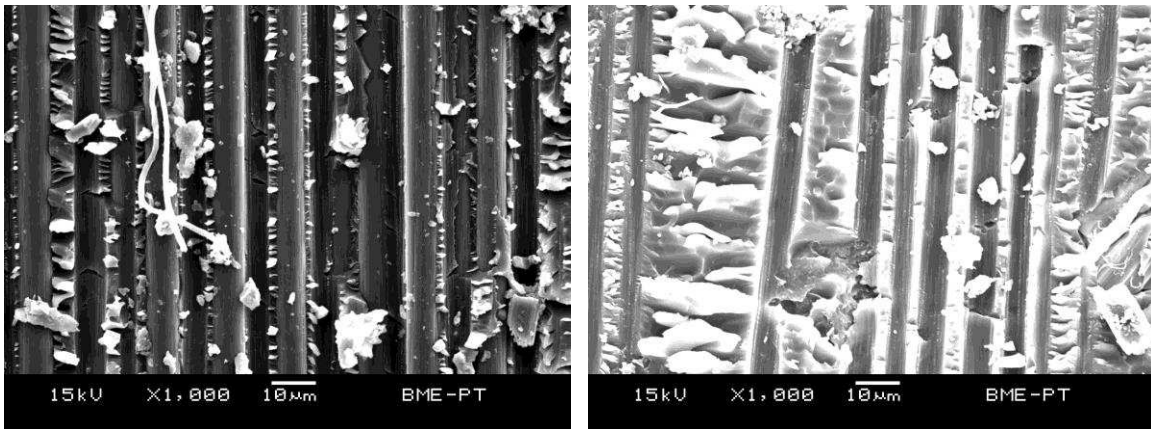


Fig. 9. SEM micrographs of the fracture surfaces of the DNS fatigue specimens (CF/EP – left, CF/MWCNT/EP – right)

Our tests results demonstrated that the DNS test setup is applicable for fatigue testing, the results are similar to the results obtained with the previously used ENF setup, and the deviations of the individual points from the average are also similar. If no buckling occurs, the DNS test setup is much easier to use and it provides a clear Mode II interlaminar shear load to the interface.

4. Conclusions

The interfacial properties of a conventional CF/EP composite system, and a CF/MWCNT/EP hybrid nanocomposite system, which showed different failure behaviors, have been compared. Static DNS and ENF tests were performed as references, to serve as a baseline for the fatigue tests and to define the static failure load levels. The static test results showed that the hybrid composites provided higher interlaminar strength compared to the classic composite system. Interlaminar fatigue behavior has been characterized with a standard ENF test and a novel implementation of the DNS test for fatigue applications. The results of both fatigue tests showed the beneficial effect of the nanofiller. While there was no significant

difference in the cycles to failure data of the ENF tests, the structural integrity, the remaining stiffness of the specimens was far better after the tests in the case of the hybrid systems. In the DNS fatigue tests the effect of the MWCNT reinforcement was more pronounced: the maximum stress-cycles to failure curve moved in the higher cycles to failure direction, showing better fatigue resistance. The fracture surfaces of the specimens of each test were examined by SEM. The results of the morphological characterization of the fracture surfaces provided a deeper understanding of the fracture phenomena. In case of the static ENF tests by the inclusion of the MWCNTs the matrix was significantly stiffened, much higher energy had to concentrate at the crack tip for the crack to propagate, resulting in an increase of the distance of the ridges representing each crack jump. In case of the fatigue tests the formation and propagation of micro-cracks is the main failure phenomenon. In case of the ENF fatigue tests much more micro-cracks were formed in case of the MWCNT containing composite, which formed a complex fracture surface showing long crack paths and intersections in the propagation paths of several micro-cracks. The DNS fatigue fracture surfaces showed similar phenomena. In case of the MWCNT reinforced system a significantly finer structure, with micro-fractured matrix areas is clearly present which also indicates more micro-cracks but also higher energy consumption during the fracture process.

The test results show that the DNS test can be used for the characterization of fatigue. Its application is simpler and provides new possibilities for further investigation. Further on valuable data on the interlaminar failure phenomena of hybrid nanocomposites is presented in both static and fatigue loading conditions.

Acknowledgements

This research was supported by The National Research, Development and Innovation Office (OTKA K 116070 and NVKP_16-1-2016-0046). Gábor Szabó acknowledges the financial support received through János Bolyai Scholarship of the Hungarian Academy of Sciences.

References

- [1] P. Robinson, E.S. Greenhalgh and S. Pinho. Failure Mechanisms in Polymer Matrix Composites, Woodhead Publishing. 2012.
- [2] G. Seon, A. Makeev, Y. Nikishkov, E. Lee. Effects of defects on interlaminar tensile fatigue behavior of carbon/epoxy composites. *Compos Sci Technol* 2013; 89:194.
- [3] L. Zhao, Y. Gong, J. Zhang, Y. Wang, Z. Lu, L. Peng, N. Hu. A novel interpretation of fatigue delamination growth behavior in CFRP multidirectional laminates, *Compos Sci Technol* 2016;133:79.
- [4] D. B. Maamar, Z. Ramdane. Characterization of the Mechanical Behaviour of Carbon Fiber Composite Laminate under Low Velocity Impact, *Period Polytech Mech Eng* 2016;60(3):142.
- [5] I. De Baere, W. Van Paepegem, J. Degrieck. Assessment of the interlaminar behaviour of a carbon fabric reinforced thermoplastic lap shear specimen under quasi-static and tension-tension fatigue loading. *Polym Test* 2015;32(7):1273.
- [6] K.C. Shekar, B.A. Prasad, N.E. Prasad. Interlaminar Shear Strength of Multi-walled Carbon Nanotube and Carbon Fiber Reinforced, Epoxy – Matrix Hybrid Composite. *Proc Mat Sci* 2014;6:1336.

- [7] V.C.S. Chandrasekaran, S.G. Advani, M.H. Santare. Role of processing on interlaminar shear strength enhancement of epoxy/glass fiber/multi-walled carbon nanotube hybrid composites. *Carbon* 2010;13:3692.
- [8] S.U. Khan, J.-K. Kim. Improved interlaminar shear properties of multiscale carbon fiber composites with bucky paper interleaves made from carbon nanofibers. *Carbon* 2012;50:5265.
- [9] H. Zabala, L. Aretxabaleta, G. Castillo, J. Aurrekoetxea. Dynamic 4 ENF test for a strain rate dependent mode II interlaminar fracture toughness characterization of unidirectional carbon fibre epoxy composites. *Polym Test* 2016;55:212.
- [10] H.L. Gowtham, Jayaram R. Pothnis, G. Ravikumar, N.K. Naik. Dependency of dynamic interlaminar shear strength of composites on test technique used. *Polym Test* 2015;42:151.
- [11] V. Kostopoulos, A. Kotrotsos, A. Baltopoulos, S. Tsantzalis, P. Tsokanas, T. Loutas, A.W. Bosman. Mode II fracture toughening and healing of composites using supramolecular polymer interlayers. *Express Polym Lett* 2016;10(11):914.
- [12] A. Szekrényes. Delamination fracture analysis in the GII–GIII plane using prestressed transparent composite beams. *Int J Solids Struct* 2007;44(10):3359.
- [13] ISO 14130:1997.
- [14] ASTM D 2344-16.
- [15] ASTM D 3846-08(2015).
- [16] ISO 20505:2005.
- [17] J. Schön, T. Nyman, A. Blom, H. Ansell. Numerical and experimental investigation of a composite ENF-specimen. *Eng Fract Mech* 2000;65(4):405.

- [18] L. Carreras, J. Renart, A. Turon, J. Costa, Y. Essa, F. Martin de la Escalera. An efficient methodology for the experimental characterization of mode II delamination growth under fatigue loading. *Int J Fatigue* 2017;95:185.
- [19] ASTM D 7905 / D 7905M-14(2014).